aNMJ-morph – A simple macro for rapid analysis of neuromuscular junction (NMJ) morphology

ROYAL SOCIETY OPEN SCIENCE

aNMJ-morph – A simple macro for rapid analysis of neuromuscular junction (NMJ) morphology

Journal:	*Royal Society Open Science*
Manuscript ID	RSOS-200128.R1
Article Type:	Research
Date Submitted by the Author:	20-Mar-2020
Complete List of Authors:	Minty, Gavin; University of Edinburgh, Edinburgh Medical School: Biomedical Sciences Hoppen, Alex; RWTH Aachen University, 52062 Aachen, Germany Boehm, Ines; University of Edinburgh, Edinburgh Medical School: Biomedical Sciences Alhindi, Abrar; University of Edinburgh, Edinburgh Medical School: Biomedical Sciences Gibb, Larissa; University of Edinburgh, Edinburgh Medical School: Biomedical Sciences Potter, Ellie; University of Edinburgh, Edinburgh Medical School: Biomedical Sciences Wagner, Boris; University of Edinburgh, Edinburgh Medical School: Biomedical Sciences Miller, Janice; Royal Infirmary of Edinburgh, Clinical Surgery Skipworth, Richard; Royal Infirmary of Edinburgh, Clinical Surgery Gillingwater, Thomas; University of Edinburgh, Edinburgh Medical School: Biomedical Sciences Jones, Ross; University of Edinburgh, Edinburgh Medical School: Biomedical Sciences
Subject:	neuroscience < BIOLOGY
Keywords:	Neuromuscular junction, NMJ-morph, macro, ImageJ, Fiji
Subject Category:	Biochemistry, Cellular and Molecular Biology

Author-supplied statements

Relevant information will appear here if provided.

Ethics

Does your article include research that required ethical approval or permits?:
This article does not present research with ethical considerations

Statement (if applicable):
CUST_IF_YES_ETHICS :No data available.

Data

It is a condition of publication that data, code and materials supporting your paper are made publicly available. Does your paper present new data?:
Yes

Statement (if applicable):
The aNMJ-morph macro, tutorial video, sample images and reference spreadsheets are available for download at Edinburgh DataShare: https://doi.org/10.7488/ds/2625

Conflict of interest

I/We declare we have no competing interests

Statement (if applicable):
CUST_STATE_CONFLICT :No data available.

Authors' contributions

This paper has multiple authors and our individual contributions were as below

Statement (if applicable):
GM, AH, IB and RAJ developed the aNMJ-morph macro. GM, AH, IB, AA, LG, EP, BCW, THG and RAJ performed all experiments and data analysis. All authors drafted and approved the manuscript for submission.

aNMJ-morph – A simple macro for rapid analysis of neuromuscular junction (NMJ) morphology

Gavin Minty[1,2]†

Alex Hoppen[3]†

Ines Boehm[1,2]†

Abrar Alhindi[1,2]

Larissa Gibb[1,2]

Ellie Potter[1,2]

Boris C. Wagner[1,2]

Janice Miller[4]

Richard J. E. Skipworth[4]

Thomas H. Gillingwater[1,2]

Ross A. Jones[1,2]*

[1]Edinburgh Medical School: Biomedical Sciences (Anatomy), University of Edinburgh, Edinburgh, EH8 9AG, UK

[2]Euan MacDonald Centre for Motor Neurone Disease Research, University of Edinburgh, Edinburgh EH8 9AG, UK

[3]RWTH Aachen University, 52062 Aachen, Germany

[4]Clinical Surgery, University of Edinburgh, Royal Infirmary of Edinburgh, Edinburgh, EH16 4SA, UK

†These authors contributed equally

*Corresponding author:

Ross Alexander Jones

University of Edinburgh, Old Medical School, Teviot Place, Edinburgh, EH8 9AG

E: Ross.Jones@ed.ac.uk

T: +44 (0)131 651 5207

Abstract

Background: Large-scale data analysis of synaptic morphology is becoming increasingly important to the field of neurobiological research (e.g. 'connectomics'). In particular, a detailed knowledge of neuromuscular junction (NMJ) morphology has proven to be important for understanding the form and function of synapses in both health and disease. The recent introduction of a standardized approach to morphometric analysis of the NMJ – 'NMJ-morph' – has provided the first common software platform with which to analyse and integrate NMJ data from different research laboratories. Here we describe the design and development of a novel macro – 'automated NMJ-morph' or 'aNMJ-morph' – to update and streamline the original NMJ-morph methodology. ImageJ Macro Language was used to encode the complete NMJ-morph workflow into 7 navigation windows that generate robust data for 19 individual pre-/post-synaptic variables. The aNMJ-morph scripting was first validated against reference data generated by the parent workflow to confirm data reproducibility. aNMJ-morph was then compared with the parent workflow in large-scale data analysis of original NMJ images (240 NMJs) by multiple independent investigators. *Results:* aNMJ-morph conferred a 4-fold increase in data acquisition rate compared with the parent workflow, with average analysis times reduced to approximately 1 minute per NMJ. Strong concordance was demonstrated between the 2 approaches for all 19 morphological variables, confirming the robust nature of aNMJ-morph. *Conclusions:* aNMJ-morph is a freely available and easy-to-use macro for the rapid and robust analysis of NMJ morphology and offers significant improvements in data acquisition and learning curve compared to the original NMJ-morph workflow.

Keywords

Neuromuscular junction, NMJ-morph, macro, ImageJ, Fiji

Background

Synaptic connectivity is central to the structure and functioning of the mammalian nervous system. In practice, the detailed analysis of synaptic connectivity – 'connectomics' – remains a formidable task. Even in small laboratory animals (e.g. mice, rats) that are routinely used to model human disease, the cerebral cortex may contain up to 1,700 synaptic connections per 1,500 μm^3 volume (1). Given the complexity of the central nervous system, the study of 'model synapses' has been critical to the progress of synaptic biology, with the neuromuscular junction (NMJ) – the synapse between lower motor neurone and skeletal muscle fibre – representing the paradigm example.

The importance of normal synaptic connectivity is evidenced by the multitude of neurodegenerative conditions that are underpinned by synaptic dysfunction and/or degeneration at the NMJ. For example, myasthenia gravis and its related syndromes, along with motor neuron diseases such as amyotrophic lateral sclerosis and spinal muscular atrophy, all demonstrate varying degrees of synaptic pathology at the NMJ as either a cause or consequence of the underlying disease mechanism (2-5). Finding effective treatments for these conditions ultimately depends on a greater understanding of the normal and pathological architecture of mammalian synapses, including NMJs.

Until recently however, even basic quantification of the gross cellular anatomy of the NMJ has been hampered by the lack of a standardized approach to morphometric analysis. Following the introduction of NMJ-morph in 2016 (6) – a simple but robust method for NMJ quantification – a growing number of research groups have now utilized this approach to gain important insights into a diverse range of conditions and species (7-12). For example, NMJ-morph was pivotal to the first major study on the cellular and molecular anatomy of the human neuromuscular junction (7). Here, NMJ-morph revealed in detail the unique 'nummular' morphology of the human NMJ and further demonstrated its structural stability over the lifespan, in direct contrast to age-related fragmentation of rodent NMJs. The sensitivity of NMJ-morph analysis has identified subtle changes in NMJ morphology found in Charcot-Marie-Tooth disease (8) and helped characterize NMJ degeneration in CHCHD10-encoded mitochondrial myopathy associated with motor neurone disease (9). Most recently,

NMJ-morph has been utilized in the study of human pathology, revealing that NMJs are stable in patients with cancer cachexia – the severe loss of skeletal muscle that is commonly associated with many forms of cancer (12).

At present, the two major barriers to more widespread adoption of NMJ-morph are its associated learning curve, and relatively low data throughput in real time (≈ 12 NMJs per hour). Here we present a macro update to the original NMJ-morph workflow – 'automated NMJ-morph' or 'aNMJ-morph' – to streamline and expedite data acquisition.

Results and Discussion

To support the continued uptake of NMJ-morph in the field of synaptic biology and related disciplines, we developed a macro update of the original workflow – 'aNMJ-morph'. The full version of the macro (compatible with both Windows and Mac operating systems) and supporting materials (including tutorial videos, sample images and reference spreadsheets) are freely available for download at Edinburgh DataShare (13). For a complete understanding of the individual morphological variables (and their derivations) we recommend that users of aNMJ-morph are familiar and competent with the use of the original workflow in a practical setting (6).

The standard NMJ-morph workflow utilizes ImageJ/Fiji (14) and the Binary Connectivity (15) plugin (all in the public domain) to generate data for 19 different morphological variables on confocal images of individual NMJs (6). For each image, this workflow requires the user to navigate through approximately 75 separate drop-down menus in Fiji, followed by manual input of raw data into a spreadsheet proforma (containing formulae for generating additional derived variables). The initial published estimate of throughput suggested a work rate of ≈ 30 NMJs per hour for an experienced user (6); in practice, we have found that most users are able to analyse ≈ 12 NMJs per hour (≈ 5 minutes per NMJ), though the throughput can be increased by the use of keyboard shortcuts built-in to ImageJ, and by the assignment of additional shortcuts.

In comparison, aNMJ-morph (Figure 1) streamlines the workflow into seven instruction windows and tabulates the results automatically (in the form of a .csv spreadsheet), reducing the image acquisition time to just under one and a half minutes per NMJ. In addition to the substantial time saving, one of the major advantages of aNMJ-morph is the simplicity of data acquisition. This enables the user to focus on the most critical step – accurate image thresholding – and reduces common errors resulting from data transcription and transposition (6).

To screen for any unanticipated scripting and/or technical issues arising during the development of the macro, a reference data set (of 40 NMJs) was first analyzed by a single investigator using both the original (NMJ-morph) and automated (aNMJ-morph) workflows. For this exercise, the same threshold settings were selected for both manual and automated assessments. As expected, the results of this initial validation generated near perfect correlations ($r = 0.954$ to 1.000; all $p<0.0001$; Table 1).

The fractionally lower correlation coefficients for the pre-synaptic variables ($r = 0.954$ to 0.998; Table 1) compared to the post-synaptic variables are a consequence of the manual erasing of nerve terminal axon following axonal diameter measurement. Manual input also accounted for the minor differences in endplate diameter between the two methods ($r = 0.992$; Table 1 and Figure 2E). For the number of AChR clusters ($r = 0.986$; Table 1) and its derivations (fragmentation and average area of AChR clusters), the discrepancy between NMJ-morph and aNMJ-morph was methodological (Figure 2D). In 3 of 40 endplates, the 'fill holes' function in the macro reduced the total number of clusters in each NMJ by one, due to enclosure of a single AChR cluster within another on the segmented image (Figure 2D). These occasional examples were not found to have any statistically significant effect in practice (see below).

To assess the usability of aNMJ-morph in practice, two pairs of investigators were then tasked with analysing a large volume of new NMJ images (Figure 3; Table 1) using either the original NMJ-morph workflow or the macro. Images were obtained from ongoing research projects and included NMJs from a range of both slow and fast twitch muscles (e.g. soleus and extensor digitorum longus, respectively; $n = 240$ NMJs in total). In addition, the new

images were of a different file format (.nd2, Nikon) to those used for the initial macro development (.lsm, Zeiss; see Methods) and each investigator used a different workstation and operating system (to ensure compatibility with both Windows and Mac).

As before, correlation analyses revealed strong concordance between the two approaches (NMJ-morph vs aNMJ-morph) for all variables ($r = 0.661$ to 0.982; all $p<0.0001$; Table 1). The greater range of correlation coefficients highlights the normal inter-user variability that is expected in relation to thresholding and manual data input, and is in keeping with the variability described in the original NMJ-morph workflow (6). Crucially, in relation to the counting of AChR clusters, correlations were strong between the two methods ($r = 0.937$, $p<0.0001$; Table 1), supporting this approach in the automation process (Figure 2D).

Of particular note, aNMJ-morph conferred a 4-fold increase in data acquisition rate, with average analysis time per NMJ reduced from nearly 5 and a half minutes (319 seconds) to just over 1 minute (79 seconds). In practical terms, this represents a substantial improvement in work rate and potential throughput. To enable robust comparison of different NMJ populations (e.g. muscles, animals, species, etc.) we recommend datasets of at least 30 to 40 NMJs per sample based on NMJ-morph guidelines (6); in real time, complete NMJ datasets can now be obtained in just over half an hour with aNMJ-morph, compared to around 3 hours or so previously, depending on level of proficiency with NMJ-morph. In addition, aNMJ-morph eliminates the common errors associated with manual data transfer via an automatically curated .csv file containing the 19 morphometric variables (and additional information on image size and threshold selection).

We anticipate that other research groups will now wish to trial the macro in different settings, e.g. with NMJ images acquired using different scanning parameters and/or file types. To support these adaptations, we recommend that users first validate the macro output against equivalent data generated using the original workflow (6) to confirm the functionality of the macro in different settings. We also encourage the development of machine-learning algorithms based on the existing NMJ-morph approach to further refine and improve the rate of data acquisition.

Conclusions

'Automated NMJ-morph' – 'aNMJ-morph' – is a freely available update to the existing NMJ-morph workflow, for the rapid and robust analysis of NMJ morphology. aNMJ-morph offers significant advantages over the original workflow, with a clear emphasis on accessibility and ease-of-use. It is hoped that aNMJ-morph will be of particular interest to NMJ biologists and associated researchers who are engaged in large-scale data analysis of comparative NMJ morphology.

Methods

Macro scripting and validation

A Fiji/ImageJ-based macro ('automated NMJ-morph' or 'aNMJ-morph') was first scripted using ImageJ Macro Language (IJM) (16) to encode the complete NMJ-morph workflow as described in the original manuscript (6). The full IJM-text transcription is included in Supplementary File 1. The final aNMJ-morph macro comprises 7 instruction windows and generates a spreadsheet containing data for 19 individual pre-/post-synaptic variables (Figure 1).

For the majority of operations in the NMJ-morph workflow, the IJM scripting involved straightforward coding of the correct sequence of drop-down menus and checkbox selections within Fiji. Several operations required further development to enable full automation, including the 'number of AChR clusters' and 'endplate diameter' (Figure 2).

Assessment of the 'number of AChR clusters' in the original NMJ-morph workflow involved manual counting of 'segmented particles' (Figure 2A, panels 1 to 3) in order to distinguish genuine clusters (i.e. those contributing to the endplate) from extraneous particles (e.g. adjacent endplates or background noise). For aNMJ-morph, we were able to automate this process via several additional steps in the macro scripting (Figure 2A, panels 4 to 6; Supplementary File 1). These steps involved overlaying filled particles onto the footprint of the endplate (using the 'fill holes' and 'concatenate' functions). Automated counting ('analyze particles') then returned the number of particles lying within the footprint alone (i.e. those contributing to the endplate) whilst excluding any extraneous particles.

On rare occasions (< 1 in 1000 images), the use of the 'segmented particles' function in the original NMJ-morph workflow resulted in spurious fragmentation of the endplate, with images resembling 'spider webs' or 'broken windows' (Figures 2B and 2C). In our experience, this was usually the result of poor image quality from the outset (Figure 2B); as per the original guidelines (6) we recommend that these NMJs are excluded entirely. In exceptional circumstances, aberrant segmentation is noted in images of sound quality (Figure 2C); in these instances, automated counting of clusters is not possible (measurement of other variables is unaffected, e.g. area, perimeter, etc.). To address these eventualities in the macro, an instruction window was incorporated prompting users to confirm appropriate segmentation of the image (Figure 1, window 6/7; Supplementary File 1); in circumstances of abnormal segmentation, the macro will still measure and record the other variables.

The measurement of 'endplate diameter' was the only other variable that required automation. In the original NMJ-morph workflow, the maximum linear dimension of the endplate was judged on inspection and recorded manually. In the macro, this value was obtained automatically by using the 'Feret's diameter' function in ImageJ, which provides an analogous measurement (Figure 2E; Supplementary File 1).

The only manual aspects of the original NMJ-morph workflow to be retained in the macro related to image thresholding and axon processing (Figure 1, windows 1-5/7). Accurate image thresholding is critical to the generation of robust NMJ-morph data (6) and it was crucial to retain this step under user-defined control; the original NMJ-morph manuscript (6) should be consulted for detailed instruction/discussion of image thresholding. Of note, thresholded binary images must be compared to the original raw images to confirm accurate image reproduction. Similarly, the measurement of axon diameter requires a degree of user-dependent decision making that is not compatible with simple automation, particularly in relation to NMJs of certain species e.g. human NMJs (7,12).

Two further variables are conventionally recorded as part of a complete NMJ-morph analysis – 'number of axonal inputs' and 'muscle fibre diameter'. Since both variables require independent measurement, they were not suitable for automation. Polyinnervation

(i.e. number of axonal inputs > 1) only occurs in certain specific circumstances (e.g. development, pathology) and requires careful assessment, whilst muscle fibre diameter is measured on a separate set of images (6).

During development, aNMJ-morph was compared against the original workflow by a single investigator utilizing the same image threshold settings. To assess the usability of aNMJ-morph in a wider context (different investigators, different laboratories, etc.), four different investigators trialled the two methods on a much larger image bank (see Results).

NMJ images and file types

All NMJ images used in the development and testing of the aNMJ-morph macro were obtained from previous and/or ongoing animal research projects covered by the requisite personal and project licences granted by the UK Home Office. All images were captured using Zeiss/Nikon confocal microscopes, with the file types .lsm/.nd2 respectively. The macro uses the maximum intensity projection of the corresponding z-stack, and has been validated for these file types and image formats only. For all other file types, we recommend that users first validate the macro output against equivalent data generated with the original workflow (6) before proceeding.

ImageJ/Fiji and Binary Connectivity

The macro was developed using ImageJ/Fiji software (version: 2.0.0-rc-67/1.52i / build: 1762a07c5c). The latest version of ImageJ/Fiji is freely available at https://fiji.sc (14) including instructions for download. The Binary Connectivity plugin is freely available at https://blog.bham.ac.uk/intellimic/g-landini-software (15) under the section 'Morphological Operators for ImageJ' (including instructions for installation). To manage updates, the latest version of the macro will be hosted at Edinburgh DataShare (13).

Statistical analysis

All statistical analyses were performed on GraphPad Prism software; individual statistical tests are indicated in the relevant figure legends.

Declarations:

Ethics

N/A

Consent for publication

N/A

Data availability

The aNMJ-morph macro, tutorial video, sample images and reference spreadsheets are available for download at Edinburgh DataShare: https://doi.org/10.7488/ds/2625 (13).

Competing interests

The authors have no competing interests to declare.

Funding

This work was supported by funding from Biomedical Sciences (Anatomy) at the University of Edinburgh (THG, RAJ) and a small research pump priming grant from the Royal College of Surgeons of Edinburgh (JM, RJES, RAJ). RJES is also supported by an NHS Research Scotland (NRS) clinician post. JM is also supported by Cancer Research UK.

Authors' contributions

GM, AH, IB and RAJ developed the aNMJ-morph macro. GM, AH, IB, AA, LG, EP, BCW, THG and RAJ performed all experiments and data analysis. All authors drafted and approved the manuscript for submission.

Acknowledgements

The authors are particularly grateful to Matthew Robinson for his helpful suggestions on the early development of the macro.

References

1. Kasthuri N, Hayworth KJ, Berger DR, Schalek RL, Conchello JA, Knowles-Barley S, Lee D, Vázquez-Reina A, Kaynig V, Jones TR, Roberts M, Morgan JL, Tapia TC, Seung HS, Roncal WG, Vogelstein JT, Burns R, Sussman DL, Priebe CE, Pfister H, Lichtman JW. Saturated reconstruction of a volume of neocortex. Cell 2015;162:648-661.

2. Vincent A. Unravelling the pathogenesis of myasthenia gravis. Nature Reviews Immunology 2002;2:797-804.

3. Titulaer MJ, Lang B, Verschuuren JJGM. Lambert–Eaton myasthenic syndrome: from clinical characteristics to therapeutic strategies. Lancet Neurol. 2011;10:1098-1107.

4. Engel AG, Shen X-M, Selcen D, Sine SM. Congenital myasthenic syndromes: pathogenesis, diagnosis, and treatment. Lancet Neurol. 2015;14:420-434.

5. Murray LM, Talbot K, Gillingwater TH. Review: neuromuscular synaptic vulnerability in motor neurone disease: amyotrophic lateral sclerosis and spinal muscular atrophy. Neuropathol. Appl. Neurobiol. 2010;36:133-156.

6. Jones RA, Reich CD, Dissanayake KN, Kristmundsdottir F, Findlater GS, Ribchester RR, Simmen MW, Gillingwater TH. NMJ-morph reveals principal components of synaptic morphology influencing structure–function relationships at the neuromuscular junction. Open Biol. 2016;doi.org/10.1098/rsob.160240.

7. Jones RA, Harrison C, Eaton SL, Llavero Hurtado M, Graham LC, Alkhammash L, Oladiran OA, Gale A, Lamont DJ, Simpson H, Simmen MW, Soeller C, Wishart TM, Gillingwater TH. Cellular and Molecular Anatomy of the Human Neuromuscular Junction. Cell Rep. 2017;21:1-9.

8. Cipriani S, Phan V, Médard JJ, Horvath R, Lochmüller H, Chrast R, Roos A, Spendiff S. Neuromuscular Junction Changes in a Mouse Model of Charcot-Marie-Tooth Disease Type

4C. Int. J. Mol. Sci. 2018;doi.org/10.3390/ijms19124072.

9. Genin EC, Hounoum BM, Bannwarth S, Fragaki K, Lacas-Gervais S, Mauri-Crouzet A, Lespinasse F, Neveu J, Ropert B, Augé G, Cochaud C, Lefebvre-Omar C, Bigou S, Chiot A, Mochel F, Boillée S, Lobsiger CS, Bohl D, Ricci J-E, Paquis-Flucklinger V. Mitochondrial defect in muscle precedes neuromuscular junction degeneration and motor neuron death in CHCHD10 S59L/+ mouse. Acta Neuropathol. 2019;138:123-145.

10. McMacken GM, Spendiff S, Whittaker RG, O'Connor E, Howarth RM, Boczonadi V, Horvarth R, Slater CR, Lochmüller H. Salbutamol modifies the neuromuscular junction in a mouse model of ColQ myasthenic syndrome. Hum. Mol. Genet. 2019;28:2339-2351.

11. Pigna E, Simonazzi E, Sanna K, Bernadzki KM, Proszynski T, Heil C, Palacios D, Adamo S, Moresi V. Histone deacetylase 4 protects from denervation and skeletal muscle atrophy in a murine model of amyotrophic lateral sclerosis. EBioMedicine 2019;40:717-732.

12. Boehm I, Miller J, Wishart TM, Wigmore SJ, Skipworth RJE, Jones RA, Gillingwater TH. Neuromuscular junctions are stable in patients with cancer cachexia. J. Clin. Invest. 2020;130(3):1461-1465. https://doi.org/10.1172/JCI128411.

13. Minty G, Hoppen A, Boehm I, Alhindi A, Gibb L, Potter E, Wagner B, Miller J, Skipworth R, Gillingwater T, Jones R. aNMJ-morph macro [dataset]. University of Edinburgh. 2019. https://doi.org/10.7488/ds/2625.

14. Schindelin J, Arganda-Carreras I, Frise E, et al. Fiji: an open-source platform for biological-image analysis. Nature Methods 2012;9(7):676-682. PMID 22743772. doi:10.1038/nmeth.2019.

15. Landini G. Advanced shape analysis with ImageJ. Proceedings of the Second ImageJ User and Developer Conference, Luxembourg, 6-7 Nov, 2008. p116-121. ISBN 2-919941-06-2. Plugins available from https://blog.bham.ac.uk/intellimic/g-landini-software/

16. Mutterer J and Rasband W. ImageJ Macro Language Programmer's Reference Guide v1.46d. http://imagej.nih.gov/ij.

Figure and Table Legends

Figure 1 – 'aNMJ-morph'

The 'aNMJ-morph' macro comprises 7 instruction windows that guide the user through the various stages of image analysis, and can be used for either single image or batch processing. The only manual inputs include image thresholding, axon processing (measure/erase) and confirmation of image segmentation. At completion, aNMJ-morph generates a data table containing 19 individual morphological variables, corresponding to those of the original NMJ-morph workflow; the 'number of axonal inputs' and 'muscle fibre diameter' are measured independently. 'Core variables' are shown in red typeface, 'derived variables' in blue and 'associated nerve and muscle variables' in green. Note: For single NMJ analysis, first open the image, then select the macro from the plugins. For batch processing, first open the macro, then select the image folder; the macro will automatically cycle through each image in turn to completion.

Figure 2 – Automation within aNMJ-morph

Several processes within the original NMJ-morph workflow required additional scripting to enable full automation. **A)** Automated counting of AChR clusters necessitated the exclusion of extraneous background particles. **B)** and **C)** Examples of aberrant image segmentation. These images are identified at the 'check segmentation' step of aNMJ-morph (window 6/7; Figure 1). **D)** Variation in particle number between NMJ-morph and aNMJ-morph (in this example, 5 clusters vs 4 clusters); in practice, these occasional examples of spurious counting were not found to be statistically significant. **E)** Automation of endplate diameter measurement using the Feret's diameter function in ImageJ/Fiji.

Figure 3 – NMJ-morph (manual) vs aNMJ-morph (macro)

aNMJ-morph offers a robust and expeditious alternative to the original NMJ-morph workflow. Two pairs of investigators analysed a large image bank (n = 240 NMJs) using either aNMJ-morph or the original workflow. **A)** Correlation analyses demonstrated strong

concordance between the two methods for all variables; examples of pre- and post-synaptic variables are illustrated (nerve terminal perimeter and endplate area). **B)** aNMJ-morph conferred a four-fold reduction in analysis time (≈ 1 minute per image) compared with the original workflow (≈ 5 minutes per image). Pearson correlation; **** $p < 0.0001$.

Table 1 – NMJ-morph (manual) vs aNMJ-morph (macro)

Correlation coefficients (*r*) comparing the two methods of image analysis for each variable. During the development of aNMJ-morph, a single investigator applied the two approaches using the same threshold settings (n = 40 NMJs; *Within User*). After validation, two pairs of investigators worked in real time on a large image bank using either aNMJ-morph or the original workflow (n = 240 NMJs; *Between User*). Correlation coefficients support the robust nature of the aNMJ-morph macro in a practical setting. Correlation coefficients (*r*) are Pearson for parametric variables, Spearman for non-parametric variables; $p < 0.0001$ for all correlation coefficients.

Supplementary File 1 – aNMJ-morph macro text

Full IJM-text (ImageJ Macro Language) transcription.

Table 1 – NMJ-morph (manual) vs aNMJ-morph (macro)

Morphological variable	NMJ-morph (manual) vs aNMJ-morph (macro)	
	Within User (r)	*Between User (r)*
Pre-synaptic		
1) Nerve Terminal Area (µm²)	0.998	0.892
2) Nerve Terminal Perimeter (µm)	0.994	0.875
3) Number of Terminal Branches	0.978	0.762
4) Number of Branch Points	0.987	0.740
5) Total Length of Branches (µm)	0.977	0.791
6) Average Length of Branches (µm)	0.954	0.661
7) "Complexity"	0.978	0.785
Post-synaptic		
8) AChR Area (µm²)	1.000	0.923
9) AChR Perimeter (µm)	1.000	0.858
10) Endplate Area (µm²)	1.000	0.982
11) Endplate Perimeter (µm)	1.000	0.949
12) Endplate Diameter (µm)	0.992	0.891
13) Number of AChR Clusters	0.986	0.937
14) Average Area of AChR Clusters (µm²)	0.971	0.823
15) "Fragmentation"	0.986	0.936
16) "Compactness" (%)	1.000	0.827
17) "Overlap" (%)	1.000	0.765
18) Area of Synaptic Contact (µm²)	1.000	0.914
Associated nerve and muscle		
19) Axon Diameter (µm)	0.960	0.758

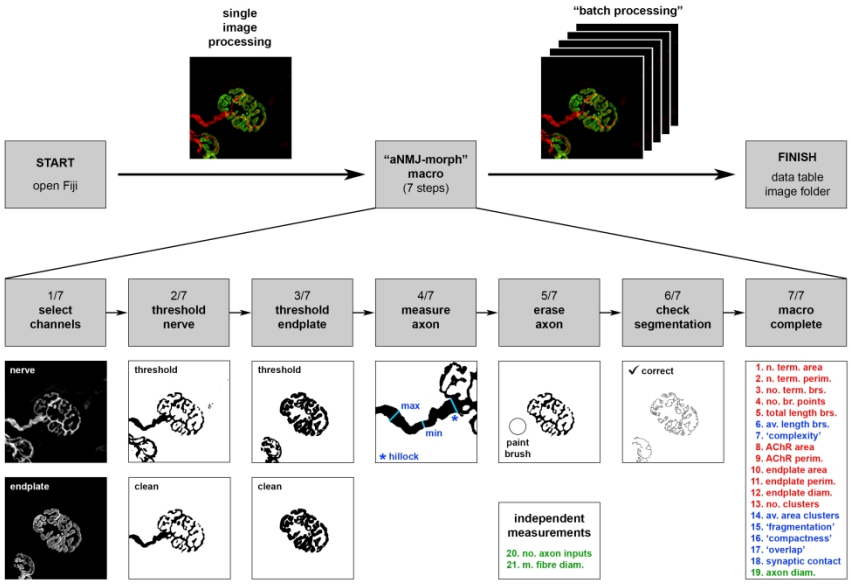
single image processing
"batch processing"
START
open Fiji
"aNMJ-morph" macro
(7 steps)
FINISH
data table
image folder
1/7 select channels
2/7 threshold nerve
3/7 threshold endplate
4/7 measure axon
5/7 erase axon
6/7 check segmentation
7/7 macro complete
nerve
threshold
threshold
max
min
hillock
paint brush
correct
1. n. term. area
2. n. term. perim.
3. no. term. brs.
4. no. br. points
5. total length brs.
6. av. length brs.
7. 'complexity'
8. AChR area
9. AChR perim.
10. endplate area
11. endplate perim.
12. endplate diam.
13. no. clusters
14. av. area clusters
15. 'fragmentation'
16. 'compactness'
17. 'overlap'
18. synaptic contact
19. axon diam.
endplate
clean
clean
independent measurements
20. no. axon inputs
21. m. fibre diam.

Figure 1

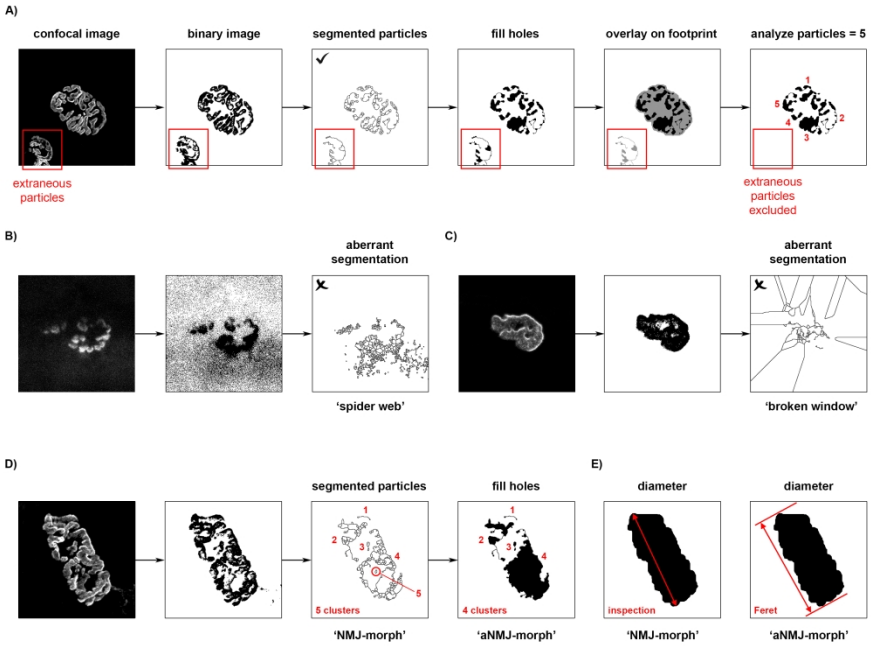
A)
confocal image
binary image
segmented particles
fill holes
overlay on footprint
analyze particles = 5
extraneous particles
extraneous particles excluded
B)
aberrant segmentation
'spider web'
C)
aberrant segmentation
'broken window'
D)
segmented particles
fill holes
5 clusters
4 clusters
'NMJ-morph'
'aNMJ-morph'
E)
diameter
diameter
inspection
Feret
'NMJ-morph'
'aNMJ-morph'

Figure 2

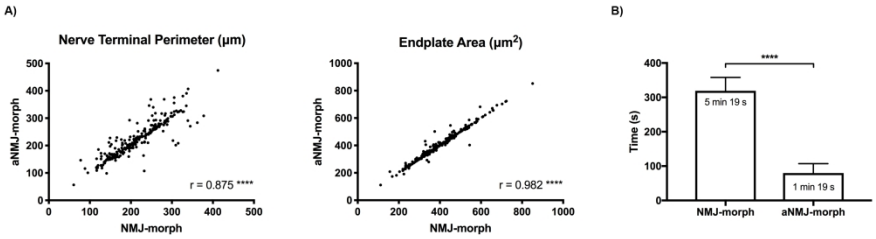
A)
Nerve Terminal Perimeter (µm)
aNMJ-morph
NMJ-morph
r = 0.875 ****
Endplate Area (µm²)
aNMJ-morph
NMJ-morph
r = 0.982 ****
B)
****
Time (s)
5 min 19 s
1 min 19 s
NMJ-morph
aNMJ-morph

Figure 3

Morphological variable	NMJ-morph (manual) vs aNMJ-morph (macro)	
	Within User (r)	*Between User (r)*
Pre-synaptic		
1) Nerve Terminal Area (µm^2)	0.998	0.892
2) Nerve Terminal Perimeter (µm)	0.994	0.875
3) Number of Terminal Branches	0.978	0.762
4) Number of Branch Points	0.987	0.740
5) Total Length of Branches (µm)	0.977	0.791
6) Average Length of Branches (µm)	0.954	0.661
7) "Complexity"	0.978	0.785
Post-synaptic		
8) AChR Area (µm^2)	1.000	0.923
9) AChR Perimeter (µm)	1.000	0.858
10) Endplate Area (µm^2)	1.000	0.982
11) Endplate Perimeter (µm)	1.000	0.949
12) Endplate Diameter (µm)	0.992	0.891
13) Number of AChR Clusters	0.986	0.937
14) Average Area of AChR Clusters (µm^2)	0.971	0.823
15) "Fragmentation"	0.986	0.936
16) "Compactness" (%)	1.000	0.827
17) "Overlap" (%)	1.000	0.765
18) Area of Synaptic Contact (µm^2)	1.000	0.914
Associated nerve and muscle		
19) Axon Diameter (µm)	0.960	0.758

ROSS A. JONES
BSc, MSc, PhD, MBChB, MRCS, FAS
Lecturer in Clinical & Surgical Anatomy
EDINBURGH MEDICAL SCHOOL: BIOMEDICAL SCIENCES
The University of Edinburgh
Old Medical School (Anatomy)
Teviot Place
Edinburgh EH8 9AG

Telephone: +44 (0)131 6515207
Email: Ross.Jones@ed.ac.uk

20 March 2020

Dear Dr Kristiansen

Re: Royal Society Open Science - Decision on Manuscript ID RSOS-200128

Thank you for your email of 16 March informing us that the above manuscript has been accepted for publication in Open Science, subject to minor revisions in accordance with the referees' suggestions. We are very grateful for the critical appraisal and valuable feedback that has been provided and welcome the opportunity to respond to the referees' comments.

We believe that our updated manuscript has now addressed all of the reviewers' remarks. Full details of the changes can be found in the specific responses to the referees' comments below. All changes to the manuscript have been highlighted in blue font and marked in grey. We hope that you find these revisions to be satisfactory.

Once again, we are delighted that our manuscript has been accepted for publication in Royal Society Open Science.

Yours faithfully

Ross A Jones
(on behalf of all co-authors)

Response from Authors (Open Science manuscript RSOS-200128)

We are very grateful to the referees for providing constructive feedback on the original manuscript. We believe that the manuscript has been improved by addressing the issues highlighted. Please find below a point-by-point response to each of the individual comments, along with details of changes and additions to the manuscript.

Responses to Reviewer Comments to the Author(s)

Reviewer: 1

This, aNMJ-morph macro, is an important improvement of an existing method to increase the time and congruence of analyzing NMJs. Despite the improvements, there is little mention of how the macro would perform with images of NMJs acquired using different scanning parameters, a critical consideration. There is also little mention if machine-learning algorithms could potentially outperform this macro and importantly be a more reliable and speedier method for assessing the morphology of NMJs taken using scanning parameters. Thus, the discussion should at least elaborate on this potential issue and future improvements.

Response: Many thanks indeed for the very positive comments. The points raised are valid and important, and we have included the following additional text in the Results and Discussion:

"We anticipate that other research groups will now wish to trial the macro in different settings, e.g. with NMJ images acquired using different scanning parameters and/or file types. To support these adaptations, we recommend that users first validate the macro output against equivalent data generated using the original workflow (6) to confirm the functionality of the macro in different settings. We also encourage the development of machine-learning algorithms based on the existing NMJ-morph approach to further refine and improve the rate of data acquisition."

Reviewer: 2

The manuscript RSOS-200128 by Gavin Minty et al. describes the novel macro for semi-automated morphometric analysis of the confocal microscopy images of neuromuscular junctions. This macro-based analysis is a development of the manual workflow that this group published in 2016. The novel macro seems useful for the field, and the authors are making the software freely available. The manuscript is interesting and seems suitable for this journal; however, several points need to be addressed. Detailed review critiques are described below in the order of appearance and not by importance.

Response: Many thanks indeed for the very positive comments.

Page 3, lines 31 to 35, "aNMJ-morph conferred a 5-fold increase in data acquisition rate compared with the parent workflow, with average analysis times reduced to approximately 1 minute per NMJ" is an over-interpretation and needs revision.
Response: We agree that the value of 5-fold is misleading in relation to the values given on the bar chart in Figure 3 (and as noted in the comments below). We have therefore replaced "5-fold" with "4-fold" throughout the manuscript.

Page 7, lines 19 to 22, "average analysis time per NMJ reduced from nearly 5 and a half minutes (319 seconds) to just over 1 minute (79 seconds)." This improvement is only four-fold (319/79=4.04).
Response: As above – "5-fold" replaced with "4-fold".

The same issue is seen on page 14, lines 54 to 58 (319/79=4.04).
Response: As above – "5-fold" replaced with "4-fold".

The same issue applies to page 6, line 3, "the image acquisition time to ≈ 1 minute per NMJ" seems like an overstatement of the difference.
Response: Following from above, we have now substituted the phrase "just under one and a half minutes".

Page 5, line 38.
Instructions should be given where to obtain the required plugin "the Binary Connectivity plugin" and how to install it.
Response: We have now included an additional section in the Methods as follows:

"ImageJ/Fiji and Binary Connectivity
The macro was developed using ImageJ/Fiji software (version: 2.0.0-rc-67/1.52i / build: 1762a07c5c). The latest version of ImageJ/Fiji is freely available at https://fiji.sc including instructions for download. The Binary Connectivity plugin is freely available at https://blog.bham.ac.uk/intellimic/g-landini-software under the section 'Morphological Operators for ImageJ' (including instructions for installation). To manage updates, the latest version of the macro will be hosted at Edinburgh DataShare (13)."

Page 6, lines 53-57.
Has the macro been tested in both Windows or Macintosh platforms? If not, authors should specify which operating system has been used for testing the macro.
Response: We can confirm that the macro has been tested and functions on both Microsoft Windows and Apple Mac operating systems. We have therefore added the following text at the relevant points in the Results and Discussion:

"…compatible with both Windows and Mac operating systems…"

"…each investigator used a different workstation and operating system (to ensure compatibility with both Windows and Mac)…"

Page 8, Methods.
Describe the Fiji version number, the Fiji build number, and the manage update sites that are necessary to execute this workflow.
Response: We have now included an additional section in the Methods as follows:

"ImageJ/Fiji and Binary Connectivity
The macro was developed using ImageJ/Fiji software (version: 2.0.0-rc-67/1.52i / build: 1762a07c5c). The latest version of ImageJ/Fiji is freely available at https://fiji.sc including instructions for download. The Binary Connectivity plugin is freely available at https://blog.bham.ac.uk/intellimic/g-landini-software under the section 'Morphological Operators for ImageJ' (including instructions for installation). To manage updates, the latest version of the macro will be hosted at Edinburgh DataShare (13)."

Page 8, lines 52 to 57. The Reviewer agrees to the authors for figure 2B being poor image quality. However, for figure 2C, the thresholding has been appropriately executed without evident noise in the image. Thus, the Reviewer disagrees with concluding this analysis problem as a result of poor image quality. The authors need to investigate the cause further and how to deal with this kind of situation. Most importantly, the Reviewer disagrees with excluding NMJs like this image from the analysis.
Response: We also agree that the thresholding in 2C is appropriate for this particular image, which nevertheless segments in the abnormal manner depicted. Having excluded poor image

quality, we can only attribute the aberrant segmentation in this particular instance to a glitch in ImageJ. In our experience, this is extremely rare (<1 in 1,000 images). In these circumstances, variables related to segmentation (i.e. number of clusters and derivations) must be necessarily excluded (hence the 'check segmentation' window in the macro) – all other variable (e.g. areas, perimeters, etc.) can of course be measured and included. We have therefore added the following text to clarify:

"…In exceptional circumstances, aberrant segmentation is noted in images of sound quality (Figure 2C); in these instances, automated counting of clusters is not possible (measurement of other variables is unaffected, e.g. area, perimeter, etc.). To address these eventualities in the macro, an instruction window was incorporated prompting users to confirm appropriate segmentation of the image (Figure 1, window 6/7; Supplementary File 1); in circumstances of abnormal segmentation, the macro will still measure and record the other variables…"

Page 9, lines 23 to 25.
The authors should describe in detail about thresholding, whether it is appropriate to use the same or different thresholding for each NMJ image.
Response: We agree that accurate image thresholding is the most critical aspect of NMJ-morph and this is discussed extensively in the original manuscript (Jones et al, 2016). We have therefore added the following text in the Methods:

"…the original NMJ-morph manuscript (6) should be consulted for detailed instruction/discussion of image thresholding. Of note, thresholded binary images must be compared to the original raw images to confirm accurate image reproduction."

Page 9, line 38, "the were" should be corrected.
Response: Thank you for noting – we have made this correction.

Page 10, lines 3 to 9, "NMJ images."
The authors must elaborate on the images used in this macro. What image file-type would be acceptable for the analysis? Which microscope manufacture original file type could be used directly in this workflow? Do the users need to load additional Fiji plugins to read specific file types necessary for the aNMJ-morph?

AND

If not, specify which file type is compatible. The Reviewer assumes that the confocal Z-stack needs to be projected. If so, specify what type of projection is suitable for this analysis?

Response: (Both comments) Thank you for raising these important points. We have added the following text to the Methods:

"NMJ images and file types
All images were captured using Zeiss/Nikon confocal microscopes, with the file types .lsm/.nd2 respectively. The macro uses the maximum intensity projection of the corresponding z-stack, and has been validated for these file types and image formats only. For all other file types, we recommend that users first validate the macro output against equivalent data generated with the original workflow (6) before proceeding."

Page 14, line 11, "batch processing." Instruction seems to be missing for how to batch process images.
Response: We apologise for the omission and have added the following text to the Figure 1 Legend:

"Note: For single NMJ analysis, first open the image, then select the macro from the plugins. For batch processing, first open the macro, then select the image folder; the macro will automatically cycle through each image in turn to completion."

Page 14, lines 12 to 14, "The Reviewer assumes that the confocal Z-stack needs to be projected. If so, specify what type of projection is suitable for this analysis?" Erasing the axon using a paintbrush is a manual input to the analysis. The same issue is seen on page 9, lines 19 to 23.
Response: Please see the above comments in relation to file types and image formats (additional text has now been added to the manuscript). We have also updated the relevant text in relation to axon processing:

(in Legends) "…The only manual inputs include image thresholding, axon processing (measure/erase) and confirmation of image segmentation…"

(in Methods) "…The only manual aspects of the original NMJ-morph workflow to be retained in the macro related to image thresholding and axon processing (Figure 1, windows 1-5/7)…"

Reviewer: 3

This is a methods paper aimed at improving the workflow in the morphological analyses of the neuromuscular synapse. Mapping the morphology of neuromuscular synapses that have altered in different species, and inferring such changes to the human neuromuscular synapse is a worthy challenge. This is because the shapes of neuromuscular synapses are vastly different across species (e.g. see papers by Clark Slater). Given this, it would be good to know how robust for the 19 NMJ variables how they can be adapted across species. I think the authors could easily demonstrated this – by perhaps showing some of their excellent comparative data from aged human and mouse NMJ – where they did employ these NMJ variables to compare and contrast mouse and human NMJs that they published in Cell Reports. For example, in figure 1 and 2 show the NMJs rodent (top panel) and human NMJs for the same/similar variable in the lower panel of each figure. Overall, I think is a very fine methods paper and should be of great value to those interested in assessing NMJ morphologies across a variety of pathophysiological conditions. I also as suggested by the text, visited the latest aNMJ-morph macro and the demo – trailed it for use – as this is the practical part of the paper.

Response: Many thanks indeed for the very positive comments. Trialling the macro across a range of mammalian species (e.g. mouse, human, etc.) and in different age groups is an excellent suggestion worthy of future consideration, but is beyond the scope of the present methods paper. Many thanks also for taking the time to trial the macro in a practical setting as part of the review process – we are very encouraged by the positive feedback.

Some possible suggestions for the authors to consider are:

1) When moving from a raw image to a binary image it might help to remind the user to threshold the background from the signal prior to creating a binary image.
Response: This is a good point. As per the original NMJ-morph guidelines, thresholding should always be performed with reference to a duplicate copy of the original image, and we have therefore added the following text to the Methods:

"…Of note, thresholded binary images must be compared to the original raw images to confirm accurate image reproduction."

2) Might be helpful for the demo to include some instruction on how to move around the image – either remind the user to place the mouse curser to the area they wanted to zoom in or the demo can remind users to use the scrolling tool.

Response: These are excellent suggestions that we will aim to include on future versions of the demo tutorial video.

3) Set escape at any step point so the user can exit the marco at any time.
Response: Apologies for any confusion - the macro can already be exited at any time by pressing escape (see hint in window 2/7 of macro). We will aim to make this point more explicit on future versions of the demo tutorial video.

4) It might be good to include some exception catching in the script to avoid problems or crashes. Researchers might make mistakes while they are operating the marco or ImageJ or even the image file itself might cause a problem. It is wise to catch those problems by setting up exception measures to make sure the inputs are appropriate. Users might not be able to spot an error on their own or they just simply misunderstand how to use aNMJ-morph or ImageJ.
Response: This is an excellent suggestion for future versions of the macro, but is beyond the scope of our programming/scripting expertise at the present time; we will aim to incorporate this functionality in future macro updates at Edinburgh DataShare. Similarly, the authors welcome any further comments and suggestions for improvements from users of the workflow/macro. A full understanding of NMJ-morph is a pre-requisite for use of the macro, especially in relation to error identification, and as stated in the manuscript "…we recommend that users of aNMJ-morph are familiar and competent with the use of the original workflow in a practical setting (6)."